Toward Autonomous Free-Climbing Robots

Tim Bretl[1], Jean-Claude Latombe[2], and Stephen Rock[1]

[1] Aerospace Robotics Lab, Department of Aeronautics and Astronautics
{tbretl,rock}@stanford.edu http://arl.stanford.edu/∼tbretl
[2] Robotics Laboratory, Computer Science Department
latombe@cs.stanford.edu http://robotics.stanford.edu/∼latombe
Stanford University, Stanford, CA, 94305, USA

Abstract. The goal of this research is to enable multi-limbed robots to climb vertical rock using techniques similar to those developed by human climbers. This paper first considers a planar three-limbed robot, then a 3-D four-limbed robot modeled after a real hardware system. It describes a fast planner based on an efficient test of the quasi-static equilibrium of these robots to compute one-step climbing moves. The planner is demonstrated in simulation for both robots.

1 Introduction

Our goal is to develop generic control, planning, and sensing capabilities to enable a wide class of multi-limbed robots to climb vertical natural terrain. We focus on "free-climbing" techniques (see Fig. 1a), where the climber only uses natural features and friction of the terrain for upward progress. These techniques are in contrast to "aid climbing", where the climber relies on additional gear [6].

The availability of non-specific autonomous rock-climbing robots could benefit several application areas. These include search-and-rescue in mountainous terrain or broken urban environments, exploration of sub-surface environments such as caves, and planetary exploration, particularly on Mars where sites with potentially high science value have been identified on cliff faces. This research may also yield the discovery of new modes of mobility for limbed robots. Indeed, human climbers often report on discovering "new degrees of freedom" providing increased balance and range of movement in everyday activity.

The robots we consider consist of a small number of articulated limbs attached to a pelvis (see Fig. 1b). Only the limb end-points make contact with the environment—a vertical surface with small, arbitrarily distributed features (e.g., protrusions, holes) called *holds*. A path through this environment is a sequence of *one-step climbing moves* in which the robot brings a limb end-point to a new hold. The robot maintains balance during each move by pushing and/or pulling at other holds, exploiting contact and friction while adjusting internal degrees of freedom (DOF's) to avoid sliding.

This paper focuses on computing one-step climbing moves. Motion is assumed quasi-static, as is usually the case in human climbing. Section 3 considers a planar three-limbed robot, and Section 4 a more complex 3-D four-limbed robot.

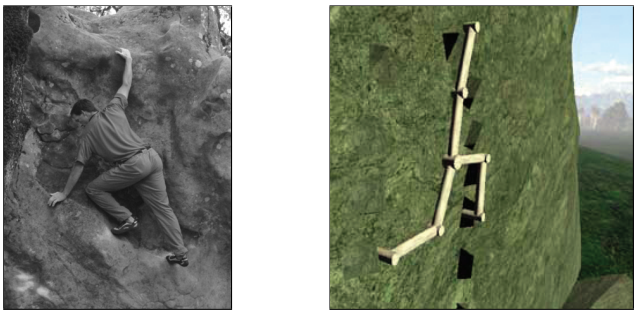

(a) Human “high-step” (b) Three-limbed robot “back-step”

Fig. 1. Typical configurations of human and robotic climbers.

2 Previous Related Work

Climbing robots. Wheeled and track rovers have been able to ascend natural slopes of up to 50 degrees and climb over small obstacles, by using techniques such as deformable tracks and active or rocker-bogie suspension [10]. Similar results have been demonstrated on legged robots [9] and snake-like robots [19] using predefined reactive gaits. Various robots capable of climbing particular vertical surfaces have also been proposed. These include robots that “stick” to a featureless, flat or smoothly curved surface by using specific end-effectors (e.g., suction cups and pads, or magnets [8]), robots whose end-effectors match engineered features of the environment (e.g., pegs [2], handrails or bars [1]), and robots designed to climb within pipes and ducts [16].

Motion planning. Few works consider the problem of careful foot-placement for multi-limbed robots, which is necessary on steep, irregular terrain. Those that do make assumptions that are not valid for climbing vertical terrain (e.g., massless legs, frictionless surfaces, strictly horizontal foot-placements) [4,14,15]. For example, the equilibrium of a planar three-limbed robot making frictional contact with its environment is studied in [15] under the assumption that the robot’s center of mass stays at the robot’s center (the point where the three limbs meet). This assumption is not realistic in practice, as limbs usually carry a significant fraction of the robot’s weight. In fact, human climbers exploit the weight of their limbs to achieve configurations that would not be in equilibrium otherwise.

Dextrous manipulation. The relationship between multi-fingered manipulation and legged locomotion has been established (e.g., in [17]). However, most algorithms for grasping objects focus on achieving force-closure [3,5], while a climbing robot need only resist gravity. Moreover, when a climbing robot’s limb moves to reach a new hold, the robot itself must remain in equilibrium during the motion as its center of mass changes. In contrast, when fingers are re-positioned on an object, the object is what needs to remain in equilibrium, but its center of mass does not change.

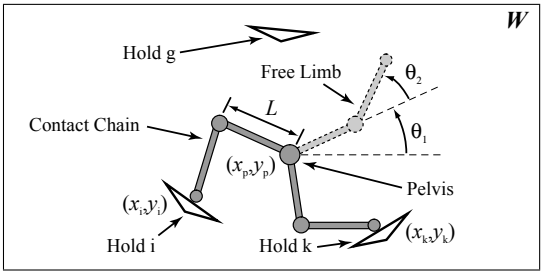

Fig. 2. Three-limbed climbing robot.

3 Planar Three-Limbed Robot

3.1 Model and problem

The robot (Fig. 2) moves in a vertical plane W. It consists of three identical limbs meeting at a point called the *pelvis*. Each limb has two links and two actuated revolute joints, one located at the pelvis, the other between the two links. We ignore self-collision. We assume all six links have equal mass and equal length L, and that joints are not limited by any internal mechanical stops. A fixed coordinate system O_{xy} is embedded in W, with gravity pointing in the negative direction of the y-axis. Any configuration of the robot is defined by 8 parameters, the coordinates (x_p, y_p) of the pelvis and the joint angles (θ_1, θ_2) of each limb.

W contains scattered *holds*. Each hold i is defined by a point (x_i, y_i) and a direction ν_i. In figures, it is depicted as an isosceles triangle; but the hold itself is located at the midpoint of the long edge of the triangle and is oriented along the outgoing normal to this edge. The endpoint of each limb is called a *foot*. In Fig. 2, two feet are at holds i and k, respectively, while the third limb is moving. The holds i and k are the *supporting* holds. The two-limbed linkage between i and k is called the *contact chain* and the other limb the *free limb*. The motion takes place in a 4-D subspace C_{ik} of the robot's configuration space, since the fixed positions of two feet at the supporting holds reduce the number of DOF's of the contact chain to 2.

Friction at each hold is modeled using Coulomb's law. If a foot is located at hold i, the reaction force $\boldsymbol{f}_i$ that the hold may exert on the foot spans a cone FC_i—the *friction cone* at i—of half-angle $\varphi_i \leq \pi/2$. The apex of this cone is at (x_i, y_i) and its main axis points along ν_i. For the robot to be in quasi-static equilibrium, there must exist reaction forces at the supporting holds whose sum exactly compensates for the gravitational force on the robot. (Henceforth, for simplicity, "equilibrium" will always mean "quasi-static equilibrium.")

We consider the following problem:

> *One-Step-Climbing Problem*. Given a start configuration q_s in C_{ik} and a hold g, compute a path of the robot connecting q_s to a configuration that places the foot of the free limb at hold g and such that the robot remains in equilibrium along the entire path.

3.2 Motion computation (basic algorithm)

Let the *feasible space* at holds i and k be the subset F_{ik} of C_{ik} where the robot is in equilibrium. We compute a solution path in F_{ik} using a PRM (Probabilistic RoadMap) planning approach [11]. The algorithm is shown below, where V and E denote the sets of vertices and edges of the roadmap, respectively, and N_1 and N_2 are parameters used to bound the computation. Note that hold g does not define a unique goal configuration. Instead, it defines a goal region that is sampled separately at Step 3. The rest of the free space F_{ik} is sampled at Step 5. Smoothing techniques are used to improve the path.

Algorithm 1 One-Step-Climbing

1. $V \leftarrow \{\}$, $E \leftarrow \{\}$
2. If q_s satisfies the equilibrium test, then add q_s to V, else exit with failure.
3. (*Sample the goal region*) Loop N_1 times:
   (a) Sample uniformly at random a combination of knee bends of the contact chain and a pelvis position (x_p, y_p) within distance $2L$ from each of the holds i, k, and g.
   (b) For each of the corresponding two configurations q where the foot of the free limb is at g, if q satisfies the equilibrium test, then add q to V.
4. If no vertex was added to V at Step 3, then exit with failure.
5. (*Sample the feasible space*) Loop N_2 times:
   (a) Sample uniformly at random a configuration $q \in C_{ik}$. If it satisfies the equilibrium test, then add q to V.
   (b) For every configuration $q' \in V$ closer to q than some predefined distance, if the linear path joining q and q' satisfies the equilibrium test, then add this path to E.
   (c) If the connected component containing q_s also contains a configuration sampled at Step 3 (goal configuration), then exit with a path.
6. Exit with failure.

3.3 Equilibrium test

The only external forces acting on the robot are gravity and the reaction forces at holds i and k. Gravity acts at the robot's center of mass (CM), the position of which varies as the robot moves. Hence, the equilibrium constraint restricts the range of positions of the CM. We specify this constraint similar to [13]. Assume that the robot has mass m, the CM is located at (x_c, y_c), and gravity is $\boldsymbol{g} = (0, -g)$. Let $\boldsymbol{r}_i = (x_i, y_i)$ and $\boldsymbol{r}_k = (x_k, y_k)$. The reaction forces at the two holds i and k are constrained to vary within friction cones FC_i and FC_k. Define unit vectors $\hat{f}_{i1}, \hat{f}_{i2}$ along each edge of FC_i. The sum of any two contact forces $\boldsymbol{f}_{i1} = f_{i1}\hat{f}_{i1}$ and $\boldsymbol{f}_{i2} = f_{i2}\hat{f}_{i2}$ lies within FC_i if and only if $f_{i1}, f_{i2} \geq 0$. So, equilibrium can be expressed as the following linear equation:

$$\begin{bmatrix} \hat{f}_{i1} & \hat{f}_{i2} & \hat{f}_{k1} & \hat{f}_{k2} & 0 & 0 \\ \boldsymbol{r}_i \times \hat{f}_{i1} & \boldsymbol{r}_i \times \hat{f}_{i2} & \boldsymbol{r}_k \times \hat{f}_{k1} & \boldsymbol{r}_k \times \hat{f}_{k2} & 0 & 0 \\ & & & & -mg & 0 \end{bmatrix} \begin{bmatrix} f_{i1} \\ f_{i2} \\ f_{k1} \\ f_{k2} \\ x_c \\ y_c \end{bmatrix} = \begin{bmatrix} 0 \\ mg \\ 0 \end{bmatrix} \tag{1}$$

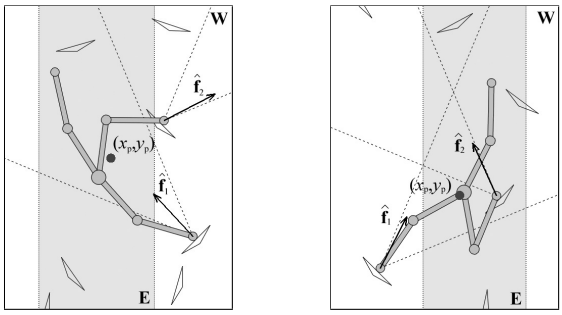

(a) Lie-back (b) Back-step

Fig. 3. Two configurations where the robot is in equilibrium.

Let E denote the set of all x_c feasible under Eq. 1, with the additional constraint that all $f_{ij}, f_{kj} \geq 0$. (Note that E is a single interval.) Eq. 1 has zero dependence on y_c, so to test a given configuration q sampled from C_{ik} for equilibrium, it suffices to check if $x_c \in E$ for this configuration. This test can be used to check a linear path between two configurations q and q' by adapting the method of [18]. Fig. 3 shows two configurations produced by our software. In each case, the column defined by E is the shaded region and the CM is the bold black dot.

3.4 Feasible space for a given configuration of the contact chain

Assume the contact chain is in a given configuration specified by the location (x_p, y_p) of the pelvis and its knee bends. Let $\Theta = \{(\theta_1, \theta_2) | \theta_1, \theta_2 \in [-\pi, \pi]\}$ denote the configuration space of the free limb and Θ_f the subset of Θ that corresponds to equilibrium configurations of the robot. Here we analyze the connectivity of Θ_f.

The abscissa x_c of the robot's CM must be in the interval $E = [x_{\min}, x_{\max}]$. Since the CM of the contact chain is fixed, this constraint can be transformed into a constraint on the CM of the free limb. Let $x_{c/chain}$ and $x_{c/free}$ denote the abscissas of the CM of the contact chain and the free limb, respectively. We have $x_{c/free} = 3x_c - 2x_{c/chain}$, so $x_{c/free}$ must lie in the interval $(x_{min/free}, x_{max/free})$, where:

$$x_{min/free} = 3x_{min} - 2x_{c/chain} \quad \text{and} \quad x_{max/free} = 3x_{max} - 2x_{c/chain} \tag{2}$$

The abscissa of the CM of the free limb can be expressed as:

$$x_{c/free} = x_p + \frac{L}{4}(3\cos\theta_1 + \cos(\theta_1 + \theta_2)) \tag{3}$$

When θ_1 and θ_2 span Θ, $\delta = x_{c/free} - x_p$ ranges between $-L$ and L. The values of θ_1 and θ_2 that are solutions of Eq. 3 for any $\delta \in [-L, L]$ define a curve in Θ. Since the mapping from (θ_1, θ_2) to Θ is single-valued, no two such curves intersect. Fig. 4a shows these curves for $\delta = -0.9L, -0.5L, 0, 0.5L$, and $0.9L$ for some configuration of the contact chain. The subset Θ_f is the region between the

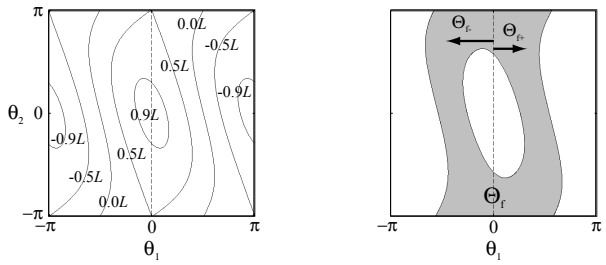

Fig. 4. Space Θ.

two curves defined by $\delta_{min} = x_{min/free} - x_p$ and $\delta_{max} = x_{max/free} - x_p$. It is shown in Fig. 4b (shaded area), where the configuration of the contact chain yields $\delta_{min} = -0.1L$ and $\delta_{max} = 0.7L$.

Θ_f is empty if and only if $[\delta_{min}, \delta_{max}] \cap [-L, L]$ is empty. So, for given knee bends of the contact chain, a pelvis location is feasible with respect to the robot's equilibrium constraint if:

$$\delta_{min} < L \quad \text{and} \quad \delta_{max} > -L \tag{4}$$

When Eq. 4 is satisfied, we divide Θ_f into two subsets: Θ_{f-}, where $\theta_1 \leq 0$ (the first link of the free limb points downward), and Θ_{f+}, where $\theta_1 \geq 0$ (the first link points upward). For any given $\delta \in [\delta_{min}, \delta_{max}] \cap [-L, L]$, the values of θ_1 and θ_2 that are solutions of Eq. 3 form a single continuous curve segment in Θ_{f-} and another one in Θ_{f+}. Since no two curves for distinct values of δ intersect, Θ_{f-} and Θ_{f+} are each connected. In addition, since $(\theta_1, \theta_2) = (-\cos^{-1}(\delta/L), 0)$ and $(\theta_1, \theta_2) = (\cos^{-1}(\delta/L), 0)$ are solutions of Eq. 3, they belong to Θ_{f-} and Θ_{f+}, respectively. So, each of the two segments defined by $\Theta_{f-} \cap \{\theta_2 = 0\}$ and $\Theta_{f+} \cap \{\theta_2 = 0\}$ span all feasible values of δ. Similarly, if two configurations (θ_1, θ_2) and (θ'_1, θ'_2) correspond to the same $\delta = \delta'$ and both belong to Θ_{f-} (resp., Θ_{f+}), a line of constant δ joining them lies entirely in Θ_{f-} (resp., Θ_{f+}).

It follows from the last statement that Θ_f is connected if and only if there exists θ_2 such that $(0, \theta_2)$ or $(\pm\pi, \theta_2)$ belongs to both Θ_{f-} and Θ_{f+}. This is the case if and only if at least one of the following conditions holds:

$$\delta_{min} \notin [-L/2, L/2] \quad \text{or} \quad \delta_{max} \notin [-L/2, L/2] \tag{5}$$

Hence, any feasible continuous path of the contact chain can be lifted into F_{ik} by letting the free limb move in either Θ_{f-} or Θ_{f+}. This yields a refined version of Alg. 1 that only samples the 2-D pelvis location space, instead of the 4-D F_{ik}.

3.5 Simulation results

Fig. 5 shows snapshots along a path computed by our planner. Frames 5b-5g show the motion along the path, during which the robot is standing on the two right-

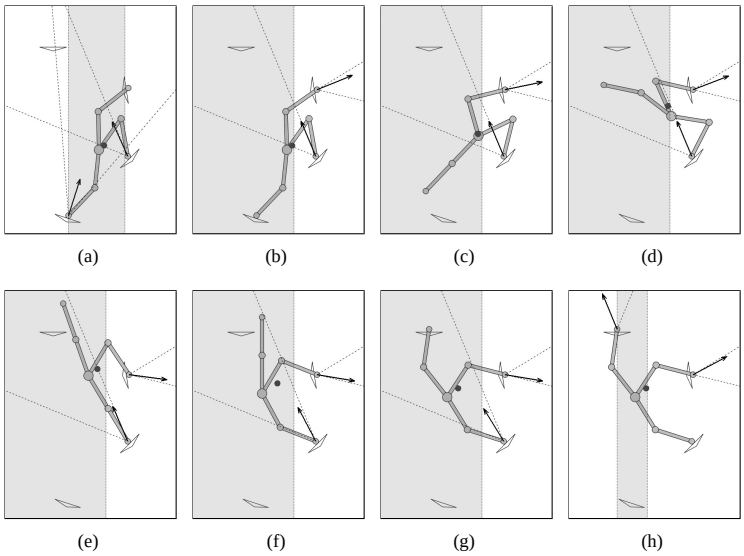

Fig. 5. Example of motion computed by Alg. 1 for the three-limbed robot.

most holds. Frames 5a and 5h show the robot configuration immediately before the transition to the initial configuration and immediately after the transition to the initial configuration of the next move. We have run the software on many examples. On average, the size of the roadmap needed to find a path is small, because F_{ij} is usually "well-connected". Narrow passages can occur in F_{ij}, but most of them exist only in the entire 4-D space, not in the 2-D space of pelvis positions. The deterministic algorithm used in the refined version of the planner for generating free limb motions allows these passages to be traversed without search.

4 3-D Four-Limbed Robot

Description of robot. In this paper we considered a robot similar to LEMUR IIb (Fig. 6 [12]), which consists of four identical limbs attached to a circular chassis. We used a slightly augmented model: each limb contains one spherical and one revolute joint (rather than three revolute), and small hooks have been added to each limb endpoint (rather than simple points), so the robot can push and pull on holds.

The robot moves in a 3-D space W. A coordinate system O_{xyz} is embedded in W, with gravity pointing in the negative direction of the z-axis. Each hold i in W is defined by a point (x_i, y_i, z_i) and a direction ν_i. During a one-step motion, three limb endpoints of the robot are in contact with supporting holds, while one limb (the free limb) is moving. The motion takes place in a 13-D space C_{ik}, since the fixed positions of three feet reduce the number of DOF's of the contact chain to 9. As in the planar case, friction at each hold is modeled using Coulomb's law. However, the robot's self-collision and collision with the environment are no longer allowed.

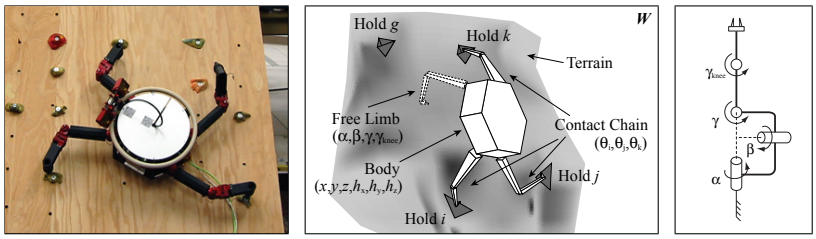

(a) LEMUR IIb (Planetary Robotics Laboratory, JPL)

(b) Model of the robot

(c) Model of each limb

Fig. 6. The 3-D four-limbed robot.

Motion computation. We currently use Alg. 1 (see Section 3.2) to plan one-step climbing moves for the 3-D robot. However, the joint limits are such that the inverse kinematics of each limb has at most one solution, so no decomposition of C_{ik} according to knee bends is needed. Also, sampling configurations of the contact chain is harder than in the planar case, so we now use a technique similar to those presented in [7]. The equilibrium test of Section 3.3 is modified as described below.

Equilibrium test. As in the planar case, the only external forces acting on the robot are gravity and the reaction forces at three holds i, j, and k. Assume that the robot has mass m, that the CM is located at (x_c, y_c, z_c), and that the gravitational force is $\boldsymbol{g} = (0, 0, -g)$. Let $\boldsymbol{r}_h = (x_h, y_h, z_h)$ for holds $h = i, j, k$. The reaction force at each hold h is constrained to vary with a friction cone FC_h. We define a conservative approximation to FC_h as an n-gonal pyramid (in our implementation, $n = 4$). Define unit vectors $\hat{f}_{h1}, \ldots, \hat{f}_{hn}$ along each edge of the pyramid. The sum of n contact forces $\boldsymbol{f}_{h1} = f_{h1}\hat{f}_{h1}, \ldots, \boldsymbol{f}_{h1} = f_{hn}\hat{f}_{hn}$ lies within the pyramid approximating FC_h if and only if $f_{h1}, \ldots, f_{hn} \geq 0$. Therefore, for each hold h, we replace the friction cone constraint on the reaction force by this linear constraint on n contact forces.

Let $\boldsymbol{f}_h = (f_{h1}, \ldots, f_{hn})$ and define the following matrix for each hold h:

$$\boldsymbol{A}_h = \begin{bmatrix} \hat{f}_{h1} & \cdots & \hat{f}_{hn} \\ \boldsymbol{r}_h \times \hat{f}_{h1} & & \boldsymbol{r}_h \times \hat{f}_{hn} \end{bmatrix} \tag{6}$$

Then the equilibrium equations can be expressed as follows:

$$\begin{bmatrix} & & & 0 & 0 & 0 \\ & & & 0 & 0 & 0 \\ & & & 0 & 0 & 0 \\ \boldsymbol{A}_i & \boldsymbol{A}_j & \boldsymbol{A}_k & 0 & -mg & 0 \\ & & & mg & 0 & 0 \\ & & & 0 & 0 & 0 \end{bmatrix} \begin{bmatrix} \boldsymbol{f}_i \\ \boldsymbol{f}_j \\ \boldsymbol{f}_k \\ x_c \\ y_c \\ z_c \end{bmatrix} = \begin{bmatrix} 0 \\ 0 \\ mg \\ 0 \\ 0 \\ 0 \end{bmatrix} \tag{7}$$

This equation has zero dependence on z_c. Let E denote the range of values of the coordinates (x_c, y_c) of the CM where the robot is in equilibrium. Finding the region

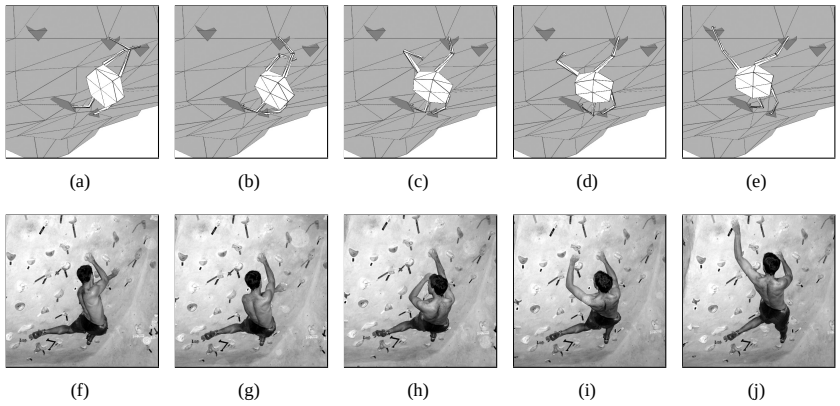

Fig. 7. Example of motion computed by Alg. 1 for the 3-D four-limbed robot.

E (which is a convex polygon) follows exactly as in Section 3.3. To test a given configuration q sampled from C_{ik} for equilibrium, we compute E and the projection (x_c, y_c) of the CM for this configuration, and check if $(x_c, y_c) \in E$.

Simulation results. Fig. 7a-7e shows snapshots of a one-step motion computed by our algorithm. In this example, the robot moves out of a "cross-through" limb position to reach for the left-most hold, on 3-D terrain with a slight overhang. During the motion, the robot rotates its pelvis, but maintains a "backstep" configuration with its two bottom limbs in order to keeps its CM within E (not shown). Fig. 7f-7j shows snapshots of a human climber executing a similar motion.

5 Future Work

This paper presented a PRM planning algorithm—One-Step-Climbing—to compute the motion of a multi-limbed robot climbing vertical terrain. The basic algorithm is fast enough to be used on-line. Nevertheless, in the case of the three-limbed robot, an analysis of the geometry of the robot's feasible space made it possible to capture narrow passages more efficiently by only sampling a subspace of the feasible space. We hope to extend this improvement to the four-limbed robot.

Applying the One-Step-Climbing algorithm in a real hardware experiment raises many other challenging problems not addressed in this paper. Sensing, grasping, and control are prominent among them. Visual and tactile sensing are needed to localize and test potential holds. Closed-loop motion control, using tactile feedback (slippage detection), should be developed to adjust computed paths during execution. Multi-step planning based on incomplete information about the terrain ahead is also needed to choose which hold to reach next, when multiple holds are within reach.

Acknowledgements. T. Bretl is partially supported by a Herbert Kunzel Fellowship. The authors would like to thank D. Halperin, T. Miller, and M. Moll for their helpful comments. In particular, they would like to thank E. Baumgartner, B. Kennedy, and H. Aghazarian of the Planetary Robotics Laboratory at JPL for their contributions.

References

1. H. Amano, K. Osuka, and T.-J. Tarn. Development of vertically moving robot with gripping handrails for fire fighting. In *IEEE/RSJ Int. Conf. on Intelligent Robots and Systems*, Maui, HI, 2001.
2. D. Bevly, S. Farritor, and S. Dubowsky. Action module planning and its application to an experimental climbing robot. In *IEEE Int. Conf. on Rob. and Aut.*, volume 4, pages 4009–4014, 2000.
3. A. Bicchi and V. Kumar. Robotic grasping and contact: A review. In *IEEE Int. Conf. on Rob. and Aut.*, pages 348–353, San Francisco, CA, 2000.
4. J.-D. Boissonnat, O. Devillers, and S. Lazard. Motion planning of legged robots. *SIAM J. on Computing*, 30(1):218–246, 2001.
5. A. V. der Stappen, C. Wentink, and M. Overmars. Computing form-closure configurations. In *IEEE Int. Conf. on Rob. and Aut.*, pages 1837–1842, 1999.
6. D. Graydon and K. Hanson. *Mountaineering: The Freedom of the Hills*. Mountaineers Books, 6th rev edition, Oct 1997.
7. L. Han and N. Amato. A kinematics-based probabilistic roadmap method for closed chain systems. In *Int. Workshop on Algorithmic Foundations of Robotics*, 2000.
8. S. Hirose, A. Nagabuko, and R. Toyama. Machine that can walk and climb on floors, walls, and ceilings. In *Int. Conf. on Advanced Robotics*, pages 753–758, Pisa, Italy, 1991.
9. S. Hirose, K. Yoneda, and H. Tsukagoshi. Titan VII: Quadruped walking and manipulating robot on a steep slope. In *IEEE Int. Conf. on Rob. and Aut.*, Albuquerque, NM, 1997.
10. K. Iagnemma, A. Rzepniewski, S. Dubowsky, P. Pirjanian, T. Huntsberger, and P. Schenker. Mobile robot kinematic reconfigurability for rough-terrain. In *Sensor Fusion and Decentralized Control in Robotic Systems III*, volume 4196 of *SPIE*, Boston, MA, 2000.
11. L. E. Kavraki, P. Svetska, J.-C. Latombe, and M. Overmars. Probabilistic roadmaps for path planning in high-dimensional configuration spaces. *IEEE Tr. on Rob. and Aut.*, 12(4):566–580, 1996.
12. B. Kennedy, H. Aghazarian, Y. Cheng, M. Garrett, G. Hickey, T. Huntsberger, L. Magnon, C. Mahoney, A. Meyer, and J. Knight. Lemur: Legged excusion mechanical utility rover. *Autonomous Robots*, 11:201–205, 2001.
13. J. Kerr and B. Roth. Analysis of multifingered hands. *Int. J. of Robotics Research*, 4(4):3–17, 1986.
14. J. J. Kuffner, Jr., K. Nishiwaki, S. Kagami, M. Inaba, and H. Inoue. Motion planning for humanoid robots under obstacle and dynamic balance constraints. In *IEEE Int. Conf. on Rob. and Aut.*, 2001.
15. A. Madhani and S. Dubowsky. The force workspace: A tool for the design and motion planning of multi-limb robotic systems. *ASME Journal of Mechanical Design*, 119(2):218–224, 1997.
16. W. Neubauer. A spider-like robot that climbs vertically in ducts or pipes. In *IEEE/RSJ/GI Int. Conf. on Intelligent Robots and Systems*, pages 1178–1185, Munich, Germany, 1994.
17. E. Rimon, S. Shoval, and A. Shapiro. Design of a quadruped robot for motion with quasistatic force constraints. *Autonomous Robots*, 10:279–296, 2001.
18. F. Schwarzer, M. Saha, and J.-C. Latombe. Exact collision checking of robot paths. In *Workshop on Algorithmic Foundations of Robotics*, Nice, France, Dec 2002.
19. M. Yim, S. Homans, and K. Roufas. Climbing with snake-robots. In *IFAC Workshop on Mobile Robot Technology*, Jejudo, Korea, 2001.